

## RADIATION RESISTANCE OF BOROSILICATE GLASS TO BETA AND GAMMA RADIATION EVALUATED USING THE ACCELERATED PROTON METHOD

Aloy A. S.<sup>1</sup>, Kovalev N. V.<sup>1</sup>, Prokoshin A. M.<sup>1</sup>, Karpovich N. F.<sup>1</sup>, Koltsova T. I.<sup>1</sup>, Gorshkov N. G.<sup>1</sup>, Kalinin V. A.<sup>1</sup>, Blokhin A. I.<sup>2</sup>, Blokhin P. A.<sup>2</sup>, Dorofeev A. N.<sup>3</sup>

<sup>1</sup>JSC V. G. Khlopin Radium Institute, St. Petersburg, Russia

<sup>2</sup>Nuclear Safety Institute of the Russian Academy of Sciences, Moscow, Russia

<sup>3</sup>State Corporation Rosatom, Moscow, Russia

Article received on February 6, 2021

*Preservation of the main physical and chemical properties of vitrified high-level waste over a long-time period under the influence of heavy radiation exposure is considered as an essential criterion for its quality assessment used to demonstrate the safety of intermediate storage under controlled conditions and subsequent final disposal of the waste. Earlier calculations covering a time period of up to  $10^4$  years allowed to identify the maximum beta- and gamma-radiation induced dose loads for borosilicate glass (BSS) of a basic composition specifically designed to vitrify liquid HLW from PDC MCC [1]. This study evaluates potential feasibility of accelerated proton beam method to simulate radiation damage according to the type of beta-gamma effects produced on the BSS and investigates their impact on its properties which is seen as a distinctive feature of this research.*

**Keywords:** radioactive waste, borosilicate glass, radiation resistance, computational modeling, absorbed dose, cyclotron.

### Introduction

There are several sources of radiation exposure acting on vitrified HLW:  $\beta$ -decay of fission products,  $\alpha$ -decay of actinides and associated  $\gamma$ -exposure [2, 3]. Radiation damage in such glasses increases along with the dose load over a span of up to  $10^6$  years and more. Under laboratory studies implemented to demonstrate the resistance of specific glass compositions to radiation exposure, the time factor can be accelerated through the use of several types of external and internal exposure.

This article discusses accelerated dose build-up cases due to external irradiation, emulating  $\beta$ - and  $\gamma$ -radiation. Interaction of  $\gamma$ -radiation with matter mainly occurs via Compton effect, photoelectric

effect and electron-positron pairing, if the energy of quanta exceeds 1.22 MeV. These interactions inevitably produce electrons in the substance with their energy levels being much higher than those of the chemical bonds in the lattice, thus, causing chemical alterations and destructive processes in the glass.  $\beta$ -ray impact on the matter results in the same effects.

Thus, there are three methods commonly used in the assessment of  $\beta$ - and  $\gamma$ -radiation effects: irradiation with a powerful electron beam in purpose-designed accelerators, transmission electron scanning (TEM/SEM) and  $\gamma$ -irradiation by  $^{60}\text{Co}$  or  $^{137}\text{Cs}$  sources.

However, long exposure time is seen as a disadvantage of the  $\gamma$ -irradiation methods involving  $^{60}\text{Co}$  or  $^{137}\text{Cs}$  sources. In case of high-capacity installations with  $^{60}\text{Co}$  irradiation generating a dose rate of some 10 Gy/s, it takes several decades for the absorbed dose to reach  $10^{10}$  Gy. Disadvantage of electron beam irradiation methods is seen in the generation and build-up of negative space charge due to the absorption of primary electrons in the sample [4]. To maintain electroneutrality, alkaline elements migrate to electron implantation points and their number in the surface layers of glass decreases; therefore, the results obtained can be influenced by chemical transformation of glass and cannot be seen as representative ones for a scenario that could describe vitrified waste aging.

Another effective method causing chemical alterations and destructive processes exists. High-energy electrons can arise during the deceleration of a proton beam at the stage of ionization deceleration. In this case, the number of emerging high-energy electrons with an energy of 5 MeV is at least three orders of magnitude higher than the number of electrons formed during the interaction of  $\beta$ - or  $\gamma$ -radiation. During intermediate collision of protons with atoms, structure of the matter is destroyed only at the very end point of their trajectory — the Bragg peak — which corresponds to the complete absorption of proton energy.

The greater is the initial kinetic energy of ions, the greater is the energy loss occurring due to ionization and the less is the one due to the stochastic interactions with nuclei. If the stage accounting for the final deceleration of particles in the matter is not considered at all, deceleration of fast particles and transfer of energy to electrons leads to the same results as the deceleration of  $\beta$ -particles or  $\gamma$ -ray scattering. Thus, electrons with their energy being significantly higher than the one of chemical bonds in the lattice are formed. This circumstance allows to study the processes of glass transformation under  $\beta$ - and  $\gamma$ -ray impact assuming accelerated simulation when the samples are bombarded with proton beams instead of  $\beta$ - and  $\gamma$ -ray irradiation.

Given these circumstances, to simulate radiation damage from high dose loads under  $\beta$ - and  $\gamma$ -exposure during the laboratory experiments, it was decided to irradiate thin glass samples of basic PDC MCC composition with a cyclotron-accelerated proton flux.

#### Irradiation with protons at MGTs-20 accelerator

For research purposes, three types of borosilicate glass have been manufactured. BS-1 glass corresponded to basic PDC MCC composition [1].

BS-2 glass contained no iron oxide, whereas the cerium oxide content was increased to 4.0 wt.% by reducing the concentration of lanthanum oxide to 2.2 wt.% as compared to BS-1 composition.

The third glass (SF-1), the composition of which is given in Table 1, was an almost pure glass frit of a basic composition, nevertheless containing no dye addition in the form of manganese oxide. When irradiated, the degree of such transparent glass darkening allowed to verify the uniformity of the absorbed dose over the part of the sample accessible to the proton beam by using a device for its scanning.

**Table 1. Chemical composition of SF-1, wt. %**

Component	Content in the glass melt, wt. %
$\text{SiO}_2$	58.76
$\text{Na}_2\text{O}$	12.89
$\text{Li}_2\text{O}$	3.61
$\text{B}_2\text{O}_3$	18.56
$\text{CaO}$	3.09
$\text{Al}_2\text{O}_3$	3.09

A beam of protons with an operating energy of 14 MeV, which were generated at the MGTs-20 cyclotron [5], was used as a radiation source. To irradiate the BSS samples, a target device was used allowing to collimate the beam on the target, to cool the target and to measure the beam current. The glass sample was installed on a substrate made of an aluminum-magnesium alloy using a clamping duralumin ring with an inner diameter of 1 cm to ensure adequate elasticity. The top of the target was additionally covered by a 50  $\mu\text{m}$ -thick aluminum foil to remove the electric charge induced by the beam of accelerated hydrogen ions and to improve sample surface cooling given extremely low thermal and electrical conductivity of the glass. Two 50  $\mu\text{m}$ -thick foils were allocated along the beam and one more was installed directly in front of the target. As a result, protons with the maximum energy ( $E_p$ ) of 12.95 MeV have impinged the target.

Seven BSS samples of different composition and thickness were irradiated at the MGTs-20 accelerator. The irradiation time of the samples amounted to 1–8 hours, the beam current accounted for  $\sim 1.5 \mu\text{A}$ . This current value was chosen as a compromise allowing to reduce the risk of surface overheating and sample cracking and to attain an acceptable dose build-up time.

The uniformity of beam distribution was ensured by raster scanning implying two U-shaped

orthogonally orientated magnets on an ion guide. Since the target station was located at a considerable distance from the cyclotron and the ultimate quadrupole lens, the beam divergence over a sample thickness of about 1 mm was neglected. In the calculations, spatial distribution of the beam on the end surface of the sample was assumed as uniform.

**Mathematical modeling of the experiment**

Mathematical modeling was implemented to identify the absorbed dose attained under the experiment. The modeling was done using PHITS [6] and RTS & T [7, 8] software and the precision statistical modeling method for coupled transport of multicomponent radiation (more than 200 types of particles and resonances) in heterogeneous spatially inhomogeneous media in a wide energy range. The approach suggested the use of libraries containing evaluated nuclear data in ENDF-6 format [9].

Figure 1 shows a cross-section of a geometric model developed for the PHITS software.

Figure 2 presents the calculated current of particles incident and passed through the target. SF-1/1 target was provided as an example. In addition to protons, the target was also hit by neutrons and photons formed as a result of an interaction between proton beam and aluminum foils.

Model BSSs of various thicknesses had a shape of disks with a radius of 0.75 cm. Table 2 presents the main characteristics of the targets and the parameters of their irradiation.

The simulation has revealed that not all targets can meet the requirement for the complete passage of the beam through them that should be complied with to simulate an accelerated build-up of the absorbed dose. Figure 3 shows the tracks of protons in the XZ section of the model representing BS-1/1 and BS-1/2 targets.

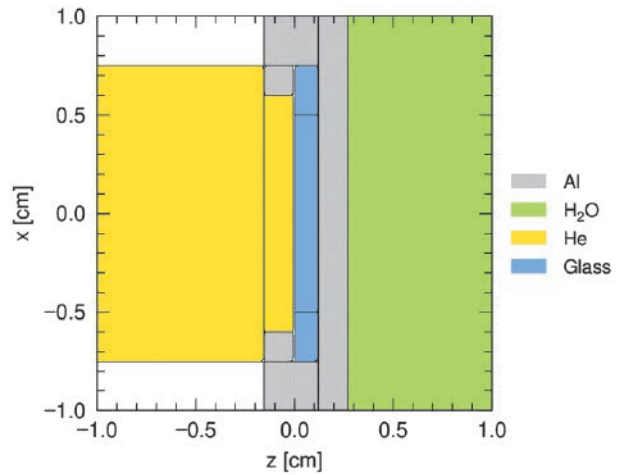


Figure 1. Model cross-section along the XZ axis

**Table 2. Characteristics of BSS model samples and parameters of their irradiation**

Sample (target)	Radius of the samples, cm	Irradiation radius of the samples, cm	Thickness of the samples, cm	Density, g/cm <sup>3</sup>	Irradiation time, h	Current, μA
BS-1/1	0.75	0.50	0.12	2.66	1.0	1
BS-1/2			0.07	2.66	4.67	1.75
BS-1/3			0.12	2.73	8.0	1.6
BS-2/1			0.09	2.66	1.0	1
BS-2/2			0.08	2.66	4.25	1.75
BS-2/3			0.11	2.66	8.0	1.9
SF-1/1			0.07	2.24	4.5	1.5

When protons pass through the target, they undergo ionization deceleration resulting in electron and photon formation with some secondary particles being generated due to nuclear reactions.

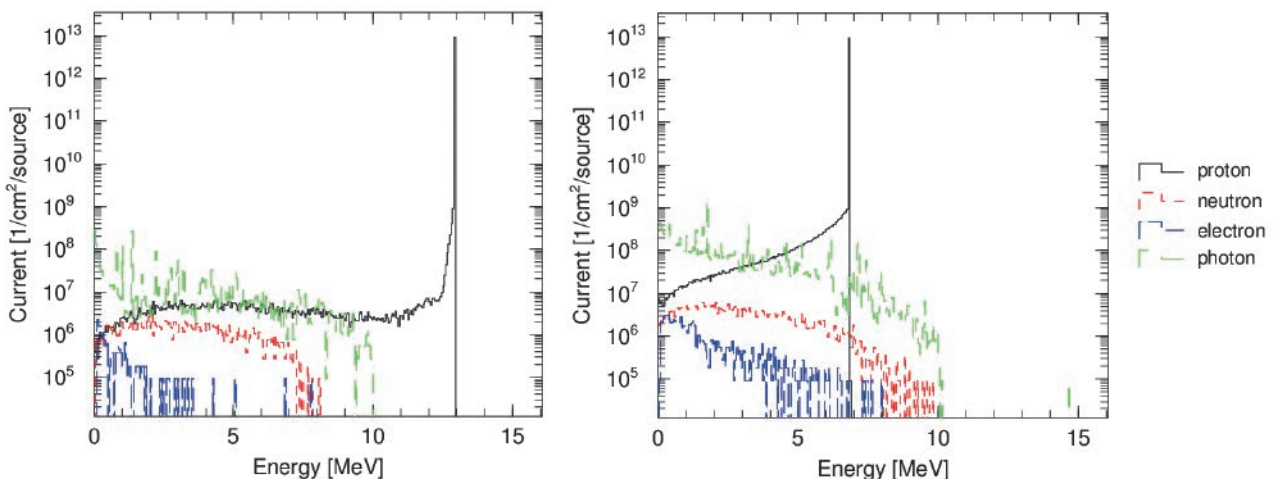


Figure 2. The current of particles incident (left) and passing through a target (right) with a diameter of 1 cm

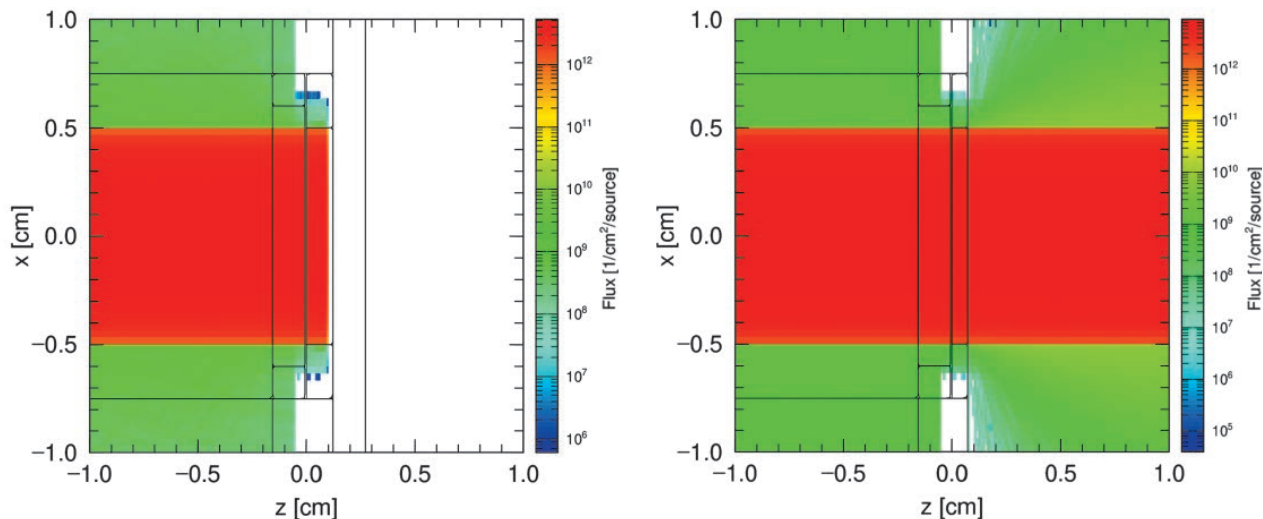


Figure 3. Protons tracks in the XZ model cross-section for targets BS-1/1 (left) and BS-1/2 (right)

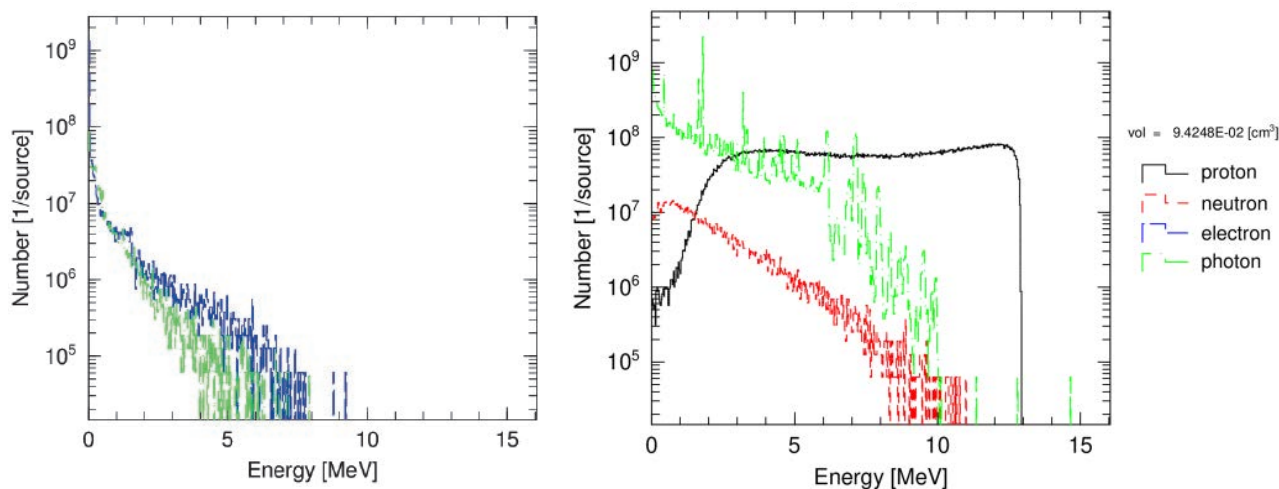


Figure 4. Energy distribution of electrons and photons, including elastic scattering, as a result of atomic interaction of protons with the target (left) and secondary particles formed due to nuclear reactions in the target (right)

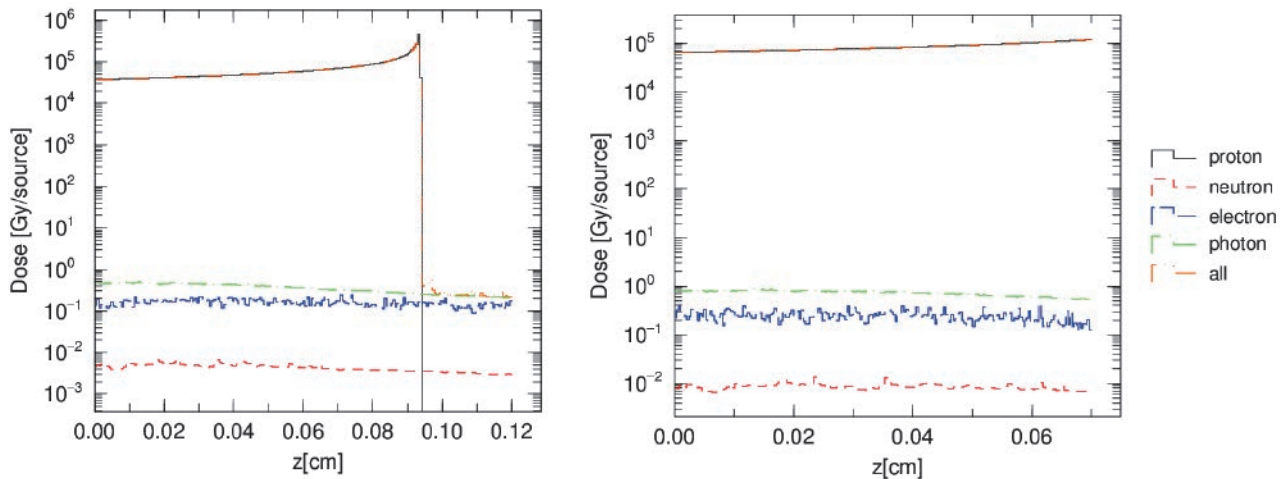
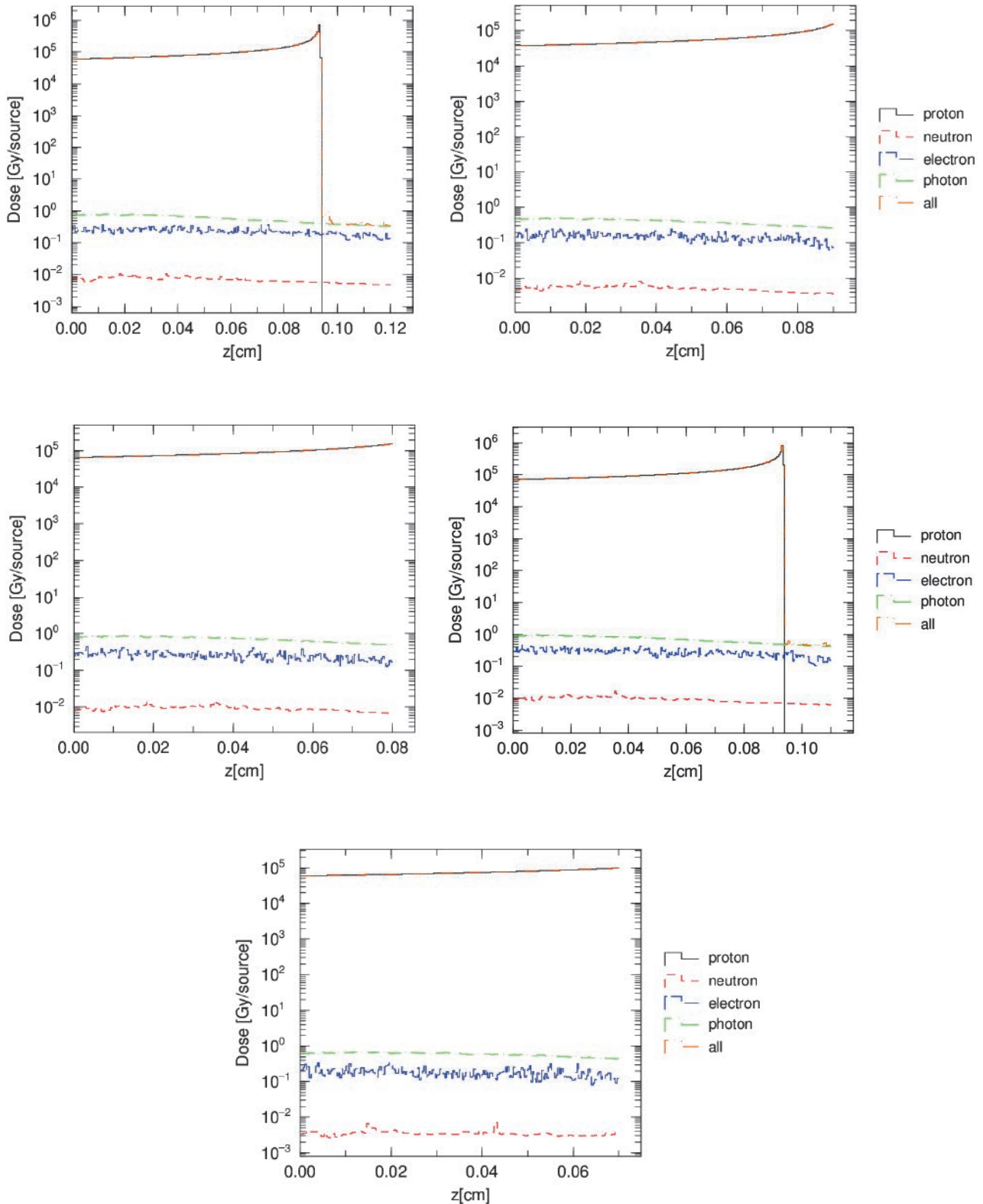


Figure 5. Distribution of absorbed doses when passed throughout the targets (BS-1/1, BS 1/2, BS 1/3, BS 2/1, BS 2/2, BS 2/3, SF 1/1) along the beam axis

## Processing, Conditioning and Transportation of Radioactive Waste



Continuation of Figure 5. Distribution of absorbed doses when passed throughout the targets (BS-1/1, BS 1/2, BS 1/3, BS 2/1, BS 2/2, BS 2/3, SF 1/1) along the beam axis

Figure 4 exemplifies the energy distribution of secondary particles formed in the BS-1/1 model target including the elastic scattering.

Figure 5 shows the distribution of the absorbed dose from different particles when they

pass through the target along the beam axis. Thus, the experiment allowed to simulate an accelerated build-up of the absorbed dose in the BS-1/2, BS-2/1, BS-2/2 and SF-1/1 targets, i. e., complete deceleration did not occur only when

the proton beam was passing through these targets.

Table 3 shows the absorbed dose for all targets resulted from ionization deceleration of protons.

**Table 3. Absorbed doses in the target during irradiation, Gy**

Glass	Calculated absorbed dose (PHITS), Gy	Conditions for $\beta$ - and $\gamma$ -radiation simulation were met
BS-1/1	$1.85 \cdot 10^8$	no
BS-1/2	$1.41 \cdot 10^9$	yes
BS-1/3	$2.37 \cdot 10^9$	no
BS-2/1	$2.08 \cdot 10^8$	yes
BS-2/2	$1.38 \cdot 10^9$	yes
BS-2/3	$3.07 \cdot 10^9$	no
SF-1/1	$1.19 \cdot 10^9$	yes

The experiment resulted in the irradiation of four glass samples corresponding to the condition assumed for  $\beta$ - and  $\gamma$ -radiation simulation. The maximum absorbed dose was found to be equal to  $1.41 \cdot 10^9$  in the BS-1/2 sample. Nevertheless, all the samples shown in Table 3 were included into the program of research focused on their post-irradiation physical and chemical properties to determine possible deterioration of BSS characteristics, in particular, water resistance due to direct collision of protons with glass atoms on a thin section of a sample exceeding the permissible thickness of 0.9 mm.

### BSS properties after its irradiation with protons

It is known that along with radiation dose build-up (due to the decay of some radionuclides)  $\beta$ - and or  $\gamma$ -radiation can lead to some alterations in the glass structure and, therefore, in its properties [10]. Before glass deformation due to water penetration starts, its structure changes and toxic elements are released into the environment, therefore, one should have a clear understanding of the irradiation effects produced on the structure of the model glass matrix intended for RW disposal.

Upon completing the irradiation, the samples were kept behind a lead shield until the dose rate did reduce to less than  $6 \mu\text{Sv/h}$ . Following the decrease in the induced activity, basic properties of BSS samples were investigated. The largest contribution to the long-lived induced  $\gamma$ -activity of glass samples with a complex chemical composition was found to be associated with such nuclides as  $^{56}\text{Co}$  and  $^{57}\text{Co}$ , as well as  $^7\text{Be}$  formed in proton-induced

reactions.  $\gamma$ -activity was measured using CANBERRA germanium semiconductor detector with GCW3023 well N<sup>o</sup>b11002 and an InSpector 2000 analyzer N<sup>o</sup> 13000180.

Density of initial BSS and of those irradiated with protons was identified according to GOST 9553-2017 by hydrostatic weighing method [11]. Table 4 shows the evaluated density of the irradiated and unirradiated samples.

**Table 4. BSS density,  $\text{g/cm}^3 \pm 1\%$**

Radiation dose, Gy	Density, $\text{g/cm}^3 \pm 1\%$	
	BS-1	BS-2
unirradiated	2.782	2.782
$10^8$	2.831	–
$(1.38 - 1.41) \times 10^9$	2.824	2.783
$(2.37 - 3.07) \times 10^9$	2.824	2.793

Table 4 demonstrates that the density of BS-1 samples under irradiation up to a dose of up to  $10^8$  Gy increases by 1.87%, whereas further increase in the dose load produces no particular changes. In case of growing dose load, the density of BS-2 samples changes within the measurement error range.

X-ray fluorescence analysis (XRF) of the samples was performed at BRUKER's D2 PHASER diffractometer using Cu radiation. The voltage of the X-ray tube was equal to 30 kV, the current amounted to 10 mA, the shooting was carried out in the range of  $2\theta$  angles ranging from  $7^\circ$  to  $70^\circ$  in the scanning mode with a step of  $0.02^\circ$  and at a rate of 0.5 deg/min. The results were processed using DIFFRAC.EVA.V5.0 software.

An X-ray amorphous halo was found to be present in the diffraction patterns of all samples (Figures 6 and 7), which testifies in favor of glassy state preservation following a high dose load impact.

Changing structure of the BSS after being irradiated with a dose of more than 10 Gy may be evidenced by the appearance of a second peak in the diffuse halo, which is apparently associated with some ordering of the glass-forming network, although the amorphous state was generally retained. The diffraction patterns for BS-2/1 and BS-2/3 glasses after their 7 months-long exposure were found to be identical to the initial BS-2 glass diffractogram. Perhaps this was due to the restoration of disturbances in the structure of the samples during the decay of the induced activity caused by new isotopes formed upon their interaction with protons.

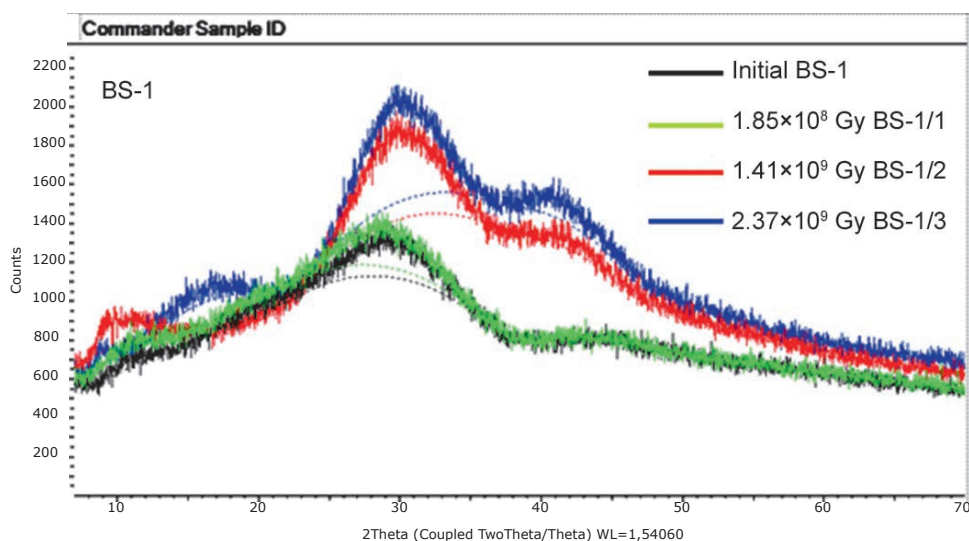


Figure 6. Diffractogram for the initial BS-1 glass and BS-1/1, BS-1/2, BS-1/3 samples with different exposure dose

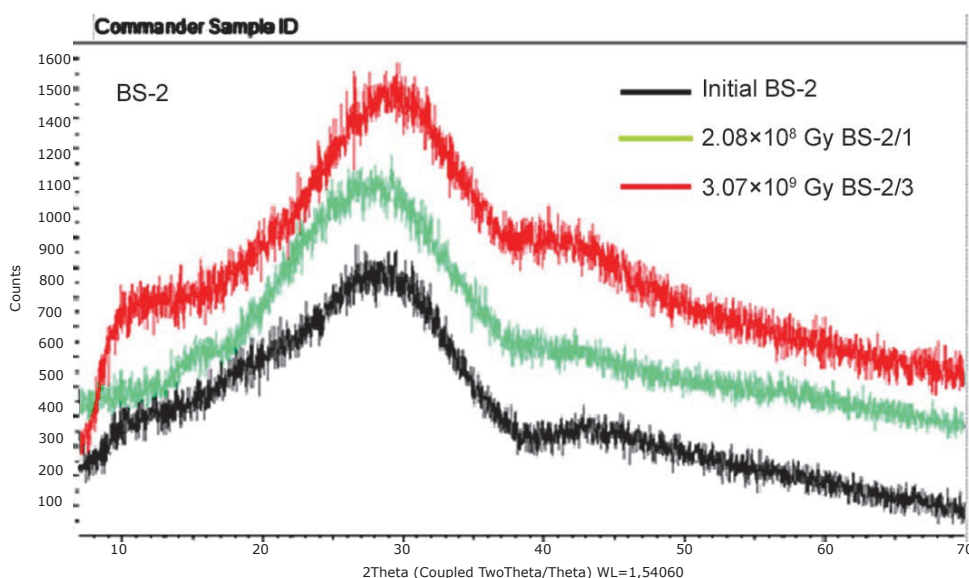


Figure 7. Diffractogram for the initial BS-2 glass and BS-2/1, BS-2/3 samples (the shooting was done following 7 months of exposure)

Water resistance of the samples was measured in accordance with GOST 52126-2003 [12]. Leaching experiments were carried out in stainless steel autoclaves at  $(90 \pm 3)^\circ\text{C}$  with temperature control in a drying cabinet implemented by VARTA TP 400 thermostat assuming possible error of  $\pm 1\%$ .

Na, Si, B and Sr concentrations in the leached elements were measured by inductively coupled plasma atomic emission spectrometry method using Varian 725 EC spectrometer (USA) with the corresponding detection limits being as follows: for Na – 4, Si – 20, B – 2 and Sr –  $0.1 \mu\text{g}/\text{dm}^3$ . Cs concentration was measured by FP-640 flame photometer (Finland) assuming a Cs detection limit of  $0.5 \text{ mg}/\text{dm}^3$ .

The edge under the clamping ring was not subject to irradiation. Table 5 shows the leaching rates at

a temperature of  $(90 \pm 3)^\circ\text{C}$  taking into account the unirradiated area under the clamping ring which accounted for  $\approx 15\%$  of the total geometric surface of the samples.

Cesium concentration in the leachate was found to be below the detection limit. Assuming a conservative approach to the assessment of cesium content at the detection limit of  $0.5 \text{ mg}/\text{l}$ , the rate of its leaching can be estimated as  $5.8 \cdot 10^{-6} \text{ g}/\text{cm}^2 \cdot \text{day}$ .

Leaching rates (Table 5) compared for non-irradiated BS-1 samples and those irradiated to a dose of  $1.41 \cdot 10^9 \text{ Gy}$  demonstrate that they remain practically constant and vary within the same order of magnitude.

The rate of component leaching from the irradiated BS-2/2 sample (up to a dose of  $1.38 \cdot 10^9 \text{ Gy}$ )

**Table 5. Leaching rates (g/cm<sup>2</sup>·day) of the components in distilled water for the studied glasses on the 28<sup>th</sup> day at a temperature of 90 ± 3 °C taking into account the unirradiated area of the sample surface (15%)**

Sample	Identified elements				
	Si	B	Na	Sr	Cs*
BS-1/1	1.7E-04	2.9E-04	2.2E-04	3.0E-05	<5.8E-06
BS-1/2	2.0E-04	3.3E-04	3.1E-04	3.9E-05	<5.8E-06
BS-1/3	2.4E-04	3.8E-04	5.2E-04	1.0E-05	<5.8E-06
BS-2/1	1.3E-05	1.7E-05	3.0E-05	4.6E-06	<5.8E-06
BS-2/2	2.9E-04	5.2E-04	4.5E-04	1.8E-05	<5.8E-06
BS-2/3	9.6E-05	1.0E-04	1.6E-04	6.4E-05	<5.8E-06

\*Calculated value if the concentration of Cs in the leach is taken equal to the detection limit of 0.5 mg/l

increases as compared to the non-irradiated BS-2 (Table 5). However, after 7 months-long leaching following the irradiation of BS-2/3 glass sample (at a dose of 3.07·10<sup>9</sup> Gy), in which, according to the calculations, the Bragg effect has manifested itself to the greatest extent, it had almost the same water resistance as the unirradiated glass.

Perhaps this indicates the ability of glass to relax internal stresses and other defects in the structure that have arisen during the irradiation.

Table 5 shows that the leaching rates for cesium and strontium radionuclides correspond to the water resistance levels with relevant standards for these elements provided in NP-019-15 with no indications regarding the temperature of the aqueous medium [13].

## Conclusion

The experimental data obtained on the main physical and chemical properties of borosilicate glass after its external β- and γ-irradiation with protons up to a dose of 3.07·10<sup>9</sup> Gy show that BS-1 glass of a basic composition maintains its structure and water resistance within ± 10% relative to its initial state.

At the same time, all BSS quality indicators following the impact of some dose loads corresponded to the values set forth in the current regulations, namely, NP-019-15, for the phosphate glass.

Based on glass sample irradiation with protons and subsequent study of their basic properties, it was experimentally found that BSS of a basic composition retains its quality at β- and γ-irradiation doses of up to 3.07·10<sup>9</sup> Gy.

## References

1. Aloy A. S., Trofimenko A. V., Kol'tsova T. I., Nikandrova M. V. Fiziko-khimicheskie kharakteristiki osteklovannykh model'nykh VAO ODTs GKHK

[Physico-Chemical Characteristics of the Vitrified Simulated HLW at EDC MCC]. *Radioaktivnye otkhody – Radioactive Waste*, 2018, no. 4 (5), pp. 67–75.

2. Aloy A. S., Kovalev N. V., Prokoshin A. M., Blokhin A. I., Blokhin P. A. et al. K voprosu ob otsenke pogloshchennoi dozy v osteklovannykh vysokoaktivnykh radioaktivnykh otkhodakh s uchetom real'noi geometrii bidonov [On the Evaluation of Absorbed Dose in Vitrified High Level Radioactive Waste with the Account of Real Can Geometry]. *Yadernaya i radiatsionnaya bezopasnost' – Nuclear and Radiation Safety*, 2020, no. 4 (98), pp. 61–72.

3. Aloy A. S., Blokhin A. I., Blokhin P. A., Kovalev N. V. Radiatsionnye kharakteristiki borosilikatnogo stekla, soderzhashchego vysokoaktivnye otkhody [Radiation Characteristics of Borosilicate Glass Containing High-Level Waste]. *Radioaktivnye otkhody – Radioactive Waste*, 2020, no. 3 (12), pp. 93–100.

4. Gin S., Jollivet P., Tribet M., Peugeot S., Schuler S. Radionuclides Containment in Nuclear Glasses: an Overview. *Radiochim. Acta*, 2017, vol. 105, no. 11, pp. 927–959.

5. Izokhronnyy tsiklotron MGTs-20 [Isochronous cyclotron MGTs-20]. URL: <http://www.niiefa.spb.su/site/right/medicine/nuclear/mgc-20> (accessed 01.08.2020).

6. Sato T., Iwamoto Y., Hashimoto S., Ogawa T. et al. Features of Particle and Heavy Ion Transport Code System PHITS Version 3.02. *J. Nucl. Sci. Technol*, 2018, vol. 55, pp. 684–690.

7. Degtyarev I. I., Novoskoltsev F. N., Liashenko O. A., Gulina E. V., Morozova L. V. RTS&T-2014 code status. *Nuclear Energy and Technology*, 2015, vol. 1, iss. 3, pp. 222–225.

8. Pryanichnikov A. A., Simakov A. S., Degtyarev I. I., Novoskoltsev F. N., Altukhova E. V., Altukhov Yu. V., Sinyukov R. Yu., Blokhin A. I. Verifikatsiya mirovykh bibliotek otsenennykh yadernykh dannykh na osnovе bazovykh integral'nykh ehksperimentov v ramkakh programmnoy kompleksa RTS&T [Verification

of the World Evaluated Nuclear Data Libraries on the Basis of Integral Experiments Using the RTS&T Code System]. *VANT, ser. Yaderno-reaktornye konstanty — Problems of Atomic Science and Technology. Series: Nuclear and Reactor Constants*, 2018, no. 1, pp. 127–136.

9. Herman M., Trkov A. ENDF-6 Formats Manual Data Formats and Procedures for the Evaluated Nuclear Data Files ENDF/B-VI and ENDF/B-VII. CSEWG Document ENDF-102 Report BNL-90365-2009 Rev. 1. URL: <https://www.oecd-nea.org/dbdata/data/manual-endf/endf102.pdf>.

10. Weber W. J., Ewing R. C., Angell C. A. et al. Radiation effects in glasses used for immobilization of high-level waste and plutonium disposition. *J. Mat. Res.*, 1997, vol. 12, no. 8, pp. 1946–1978.

11. GOST 9553-2017. Mezhsudarstvennyi standart. Steklo i izdeliya iz nego. Metod opredeleniya

plotnosti [Glass and glass products. Density determination method].

12. GOST R 52126-2003. Natsional'nyi standart Rossiiskoi Federatsii. Otkhody radioaktivnye. Opredelenie khimicheskoi ustoychivosti otverzhennykh vysokoaktivnykh otkhodov metodom dlitel'nogo vyshchelachivaniya [Radioactive waste. Long time leach testing of solidified radioactive waste forms].

13. NP-019-15. Federal'nyye normy i pravila v oblasti ispol'zovaniya atomnoy energii. Sbor, pererabotka, khraneniye i konditsionirovaniye zhidkikh radioaktivnykh otkhodov. Trebovaniya bezopasnosti [Federal norms and rules in the field of atomic energy use Collection, Processing, Storage and Conditioning of Liquid Radioactive Waste. Safety requirements].

---

### Information about the authors

*Aloy Albert Semenovich*, Doctor of Sciences, chief researcher, JSC V. G. Khlopin Radium Institute (28, 2nd Murinsky Ave., St. Petersburg, 194021, Russia), e-mail: [aloy@khlopin.ru](mailto:aloy@khlopin.ru).

*Kovalev Nikita Vladimirovich*, researcher, JSC V. G. Khlopin Radium Institute (28, 2nd Murinsky Ave., St. Petersburg, 194021, Russia), e-mail: [kovalev@khlopin.ru](mailto:kovalev@khlopin.ru).

*Prokoshin Alexander Mikhailovich*, lead engineer, JSC V. G. Khlopin Radium Institute (28, 2nd Murinsky Ave., St. Petersburg, 194021, Russia), e-mail: [a.m.prokoshin@khlopin.ru](mailto:a.m.prokoshin@khlopin.ru).

*Karpovich Natalia Fedorovna*, Ph.D., leading researcher, JSC V. G. Khlopin Radium Institute (28, 2nd Murinsky Ave., St. Petersburg, 194021, Russia), e-mail: [knf@khlopin.ru](mailto:knf@khlopin.ru).

*Koltsova Tatyana Ivanovna*, lead engineer, JSC V. G. Khlopin Radium Institute (28, 2nd Murinsky Ave., St. Petersburg, 194021, Russia), e-mail: [koltsova@khlopin.ru](mailto:koltsova@khlopin.ru).

*Gorshkov Nikolay Georgievich*, Ph.D., leading researcher, JSC V. G. Khlopin Radium Institute (28, 2nd Murinsky Ave., St. Petersburg, 194021, Russia) until December 2020.

*Kalinin Valery Anatolyevich*, Ph.D., head of laboratory, JSC V. G. Khlopin Radium Institute (28, 2nd Murinsky Ave., St. Petersburg, 194021, Russia), e-mail: [v\\_kalinin@khlopin.ru](mailto:v_kalinin@khlopin.ru).

*Blokhin Anatoly Ivanovich*, Ph.D., leading researcher, Nuclear Safety Institute of the Russian Academy of Sciences (52, Bolshaya Tuskaya st., Moscow, 115191, Russia), e-mail: [bai@ibrae.ac.ru](mailto:bai@ibrae.ac.ru).

*Blokhin Pavel Anatolievich*, Ph.D., head of laboratory, Nuclear Safety Institute of the Russian Academy of Sciences (52, Bolshaya Tuskaya st., Moscow, 115191, Russia), e-mail: [blokhin@ibrae.ac.ru](mailto:blokhin@ibrae.ac.ru).

*Dorofeev Aleksander Nikolaevich*, Ph.D., Head of the Project Office on the Development of a Unified Radioactive Waste Management System, State Corporation Rosatom (24, Bolshaya Ordynka st., Moscow, 119017, Russia), e-mail: [ANDorofeev@rosatom.ru](mailto:ANDorofeev@rosatom.ru).

### Bibliographic description

Aloy A. S., Kovalev N. V., Prokoshin A. M., Karpovich, N. F., Koltsova T. I., Gorshkov N. G., Kalinin V. A., Blokhin A. I., Blokhin P. A., Dorofeev A. N. Radiation resistance of borosilicate glass to beta and gamma radiation evaluated using the accelerated proton method. *Radioactive Waste*, 2021, no. 1 (14), pp. 8–18. DOI: 10.25283/2587-9707-2021-1-8-18. (In Russian).